# Synthesis, Crystal Structure, and Magnetic Properties of CoMoFeAl and Related Compounds

Gavin Baker[1], Jax Wysong[1], Shah Valloppilly[2], Paul Shand[3], Pavel Lukashev[3], and Parashu Kharel[1*]

*1Department of Physics, South Dakota State University, Brookings, SD 57007, USA*
*2Nebraska Center for Materials and Nanoscience, University of Nebraska, Lincoln, NE 68588, USA*
*3Department of Physics, University of Northern Iowa, Cedar Falls, IA 50614, USA*
*Corresponding author: parashu.kharel@sdstate.edu

## Abstract

We have carried out joint theoretical and experimental investigations of three Heusler compounds CoMoFeAl, $CoMo_{0.5}Fe_{1.5}Al$, and $Co_{1.5}Mo_{0.5}FeAl$. Our first-principle calculations show that all three compounds show either ferro- or ferrimagnetic order with CoMoFeAl and $CoMo_{0.5}Fe_{1.5}Al$ exhibiting high spin polarization of almost 80%. The investigated samples were prepared using arc melting and high vacuum annealing. All the samples show cubic crystal structure with disorder. The parent compound CoMoFeAl shows a small saturation magnetization of 12 emu/g, and a Curie temperature of 440K. The other two compounds, namely, $Co_{1.5}Mo_{0.5}FeAl$ and $CoMo_{0.5}Fe_{1.5}Al$, show much higher saturation magnetizations of 62 emu/g and 59 emu/g, and substantially higher Curie temperatures of 950K and 780K, respectively.

## I. Introduction

Heusler alloys have attracted significant attention due to their interesting properties such as high perpendicular magnetic anisotropy, shape memory effect, topological magnetic order, and magnetocaloric effect [1-6]. In recent years, these materials have been intensely studied due to their half-metallic or spin-gapless semiconducting properties [7]. Heusler compounds are useful for spintronic applications as they can produce fully (100%) spin polarized currents because of the nature of their electronic structure, which is metallic for one spin channel and insulating for the opposite channel [8,9]. Materials including ferro- and ferrimagnetic Heusler alloys exhibiting high Curie temperature may retain a high degree of spin polarization at room temperature making them suitable for spintronic applications [10-13]. Another important feature of Heusler alloys is that the

magnetic and electronic properties can be tuned as desired by adjusting the elemental composition, applying mechanical strain, etc. [12-15].

In general, Heusler alloys crystallize in a cubic structure, and they are classified as ternary (XYZ, $X_2YZ$) and quaternary ($XX'YZ$) alloys where X, $X'$, and Y are transition-metal elements and Z is the main-group element. The completely ordered quaternary Heusler alloys crystalize in cubic Y type ($XX'YZ$) structure (prototype LiMgPdSn) [1]. However, in experiment, most of the synthesized alloys are found to be crystallized in disordered $L2_1$, B2, or A2 structures. The $L2_1$ type disorder develops when the X and $X'$ atoms mix in the lattice, whereas the B2 type structure results from the mixing of Y and Z atoms. The A2 disorder results from a random mixing of all atoms (X, $X'$,Y, Z). These disorders are typically detrimental to the magnetic and spin-electronic properties of Heusler alloys [16].

This paper includes our combined computational and experimental study of CoMoFeAl, and the effect of deviation from stoichiometry on its magnetic and electronic band properties. In particular, we have investigated $Co_{1.5}Mo_{0.5}FeAl$ and $CoMo_{0.5}Fe_{1.5}Al$ in addition to the parent alloy and demonstrated that the magnetic properties, namely, the magnetization and Curie temperature are highly sensitive to the change in elemental composition. In addition, our computational results indicate that CoMoFeAl and $CoMo_{0.5}Fe_{1.5}Al$ in cubic structure have relatively high spin polarizations of about 80% but $Co_{1.5}Mo_{0.5}FeAl$ is essentially non-spin polarized.

## II. Methods

### a. Experimental Methods

The bulk CoMoFeAl, $Co_{1.5}Mo_{0.5}FeAl$, and $CoMo_{0.5}Fe_{1.5}Al$ alloys were synthesized using arc melting and high vacuum annealing. First, highly pure (99.99%) metal pieces with proper weight ratio were cut from corresponding commercially available pellets and melted on a water-cooled Cu hearth of the arc furnace in an argon environment, and the ingots thus produced were annealed in a tubular vacuum furnace at 950°C for 1 week. The crystal structures of the samples were studied with a Rigaku MiniFlex600 x-ray diffractometer using a Cu-Kα source ($\lambda = 1.54$Å). The magnetic properties were measured using a Quantum Design VersaLab magnetometer.

### b. Computational Methods

All calculations in this work are perfomed with the Vienna *ab initio* simulation package (VASP) [17], using the projector augmented-wave method (PAW) [18] and generalized-gradient approximation (GGA) [19]. The cut-off energy of plane-waves is set to 500 eV, and a 0.05 eV width of smearing is used within the integration method by Methfessel and Paxton [20]. The energy convergence criteria was set to $10^{-6}$ eV and $10^{-5}$ eV for electronic structure and atomic relaxations calculations, correspondingly. The Brillouin-zone integration was performed with a *k*-point mesh of 12 × 12 × 12, for a 16-atom cubic cell. The crystal structures are analyzed with the MedeA® software environment [21]. The calculations were performed using Extreme Science and Engineering Discovery Environment (XSEDE) resources located at the Pittsburgh Supercomputing Center (PSC) [22], and the resources of the Center for Functional Nanomaterials (CFN) at Brookhaven National Laboratory (BNL).

## III. Results and Discussion

### a. Computational Results

Our first principles calculations suggest that the lowest energy configuration of CoMoFeAl corresponds to the inverted cubic Heusler structure. The calculated density of states (DOS) in this structure is shown in Fig. 1(a). The calculated spin polarization (defined as $P = \frac{N_\uparrow(E_F) - N_\downarrow(E_F)}{N_\uparrow(E_F) + N_\downarrow(E_F)}$, where $N_{\uparrow,\downarrow}(E_F)$ is the spin-dependent density of states (DOS) at the Fermi level, $E_F$) is almost 80%. The magnetic alignment is ferromagnetic, where Fe and Co moments align parallel to each other exhibiting a net magnetization of 1.92 $\mu_B$ / f.u. The individual atomic moments of Co and Fe are respectively 1.15 $\mu_B$, and 0.77 $\mu_B$, with the magnetic moments of Mo and Al being negligible. The calculated lattice constant for the low energy configuration of CoMoFeAl is 5.865 Å.

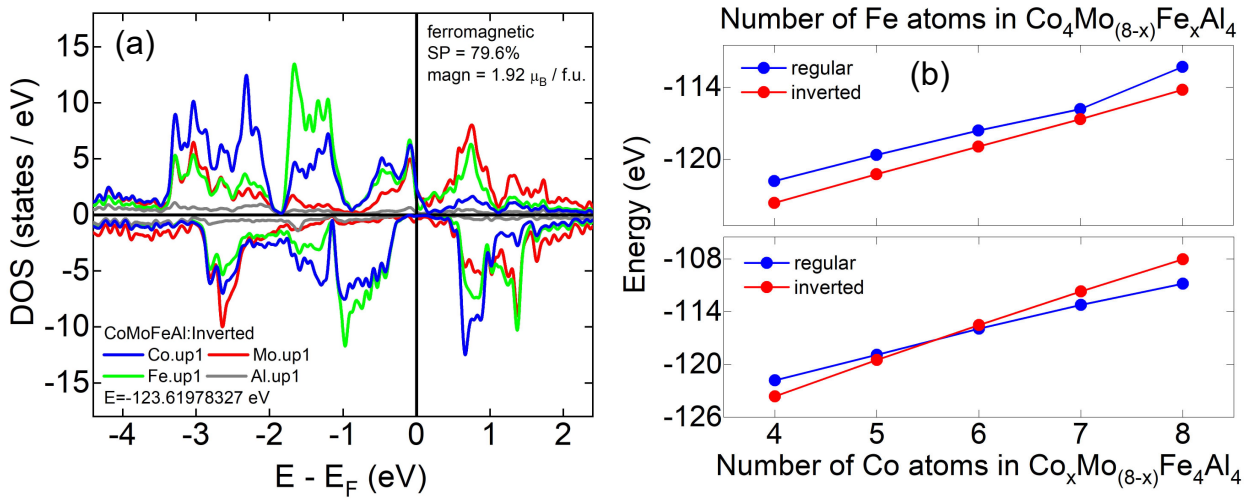


Figure 1: (a) Calculated element- and spin-resolved density of states of CoMoFeAl. Elemental contributions are colored as indicated in the figure: Co – blue, Fe – green, Mo – red, Al – brown. Positive and negative DOS represent majority- and minority-spin, correspondingly. Vertical line indicates position of the Fermi level. Calculated magnetization and spin polarization values are shown in the figure. (b) Calculated energies of $Co_4Mo_{(8-x)}Fe_xAl_4$ and $Co_xMo_{(8-x)}Fe_4Al_4$, as a function of $x$, for regular and inverted Heusler structures.

Figure 1(b) shows calculated energies of $Co_4Mo_{(8-x)}Fe_xAl_4$ and $Co_xMo_{(8-x)}Fe_4Al_4$, as a function of $x$, for regular and inverted Heusler structures. As one can see from this figure, $Co_4Mo_{(8-x)}Fe_xAl_4$ prefers to crystallize in inverted Heusler structure for all values of $x$. At the same time, while $Co_xMo_{(8-x)}Fe_4Al_4$, has lower energy in the inverted Heusler structure for $x < 6$, the regular Heusler structure becomes energetically favorable for $x > 6$. Here, $x = 6$ corresponds to our experimental sample $Co_{1.5}Mo_{0.5}FeAl$.

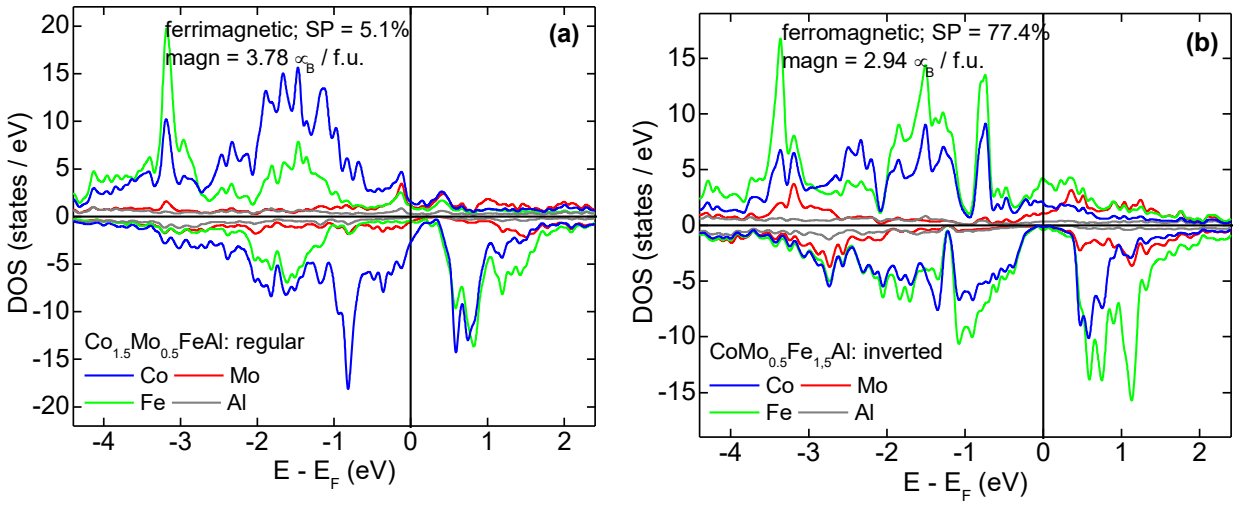


Fig. 2: Calculated element- and spin-resolved density of states of $Co_{1.5}Mo_{0.5}FeAl$ (a), and $CoMo_{0.5}Fe_{1.5}Al$ (b). Elemental contributions are colored as indicated in the figure: Co – blue, Fe – green, Mo – red, Al – brown. Positive and negative DOS represent majority- and minority-spin, correspondingly. Vertical line indicates position of the Fermi level. Calculated magnetization and spin polarization values are shown in the figure.

Figure 2 shows calculated density of states of $Co_{1.5}Mo_{0.5}FeAl$ (a) and $CoMo_{0.5}Fe_{1.5}Al$ (b). The density of states of the latter is calculated for the inverted Heusler structure since it corresponds to the minimum energy structure (see Fig. 1(b)). At the same time, as one can see from Fig. 1(b), the regular and inverted Heusler structures of $Co_{1.5}Mo_{0.5}FeAl$ have almost identical energies with the regular structure having slightly smaller energy. Therefore, we have shown the calculated DOS in the regular Heusler structure of $Co_{1.5}Mo_{0.5}FeAl$ in Fig. 2 (a). However, we have calculated the degree of spin polarization for both regular and inverted structures which are 5% and 1%, respectively. Therefore, this material may not be attractive for practical spintronic applications. On the other hand, the calculated spin polarization for $CoMo_{0.5}Fe_{1.5}Al$ is about 78 %, making it useful for spin transport-based device applications.

Both $CoMo_{0.5}Fe_{1.5}Al$ and $Co_{1.5}Mo_{0.5}FeAl$ show moderate net magnetizations of 2.94 $\mu_B$ / f.u and 3.78 $\mu_B$ / f.u, respectively, where the magnetic order for the first is ferromagnetic and that for the second is ferrimagnetic. In the latter, the ferrimagnetic alignment results from a sizable magnetic moment of Mo (0.42 $\mu_B$ / Mo) that is anti-aligned with atomic moments of Co and Fe. We note that there is a small tetragonal distortion in the structure of both compounds with a =5.764

Å, b = c = 5.786 Å for $CoMo_{0.5}Fe_{1.5}Al$, and a = 5.848 Å, b = c = 5.803 Å for $Co_{1.5}Mo_{0.5}FeAl$, respectively. However, the tetragonal distortions seen in calculation are too small to observe in real samples.

### b. Experimental Results

Figure 3 shows the room temperature x-ray diffraction (XRD) pattern of powder sample of vacuum annealed CoMoFeAl, $Co_{1.5}Mo_{0.5}FeAl$, and $CoMo_{0.5}Fe_{1.5}Al$ alloys. All three XRD patterns can be indexed with cubic structure with disorder. The lack of the (111) and (200) peaks in the patterns indicate that the sample have A2 type disorder [23]. The XRD pattern simulated using Rietveld refinement for A2 type disordered structure has a perfect match with our data. In addition, there is about 30 wt.% of Fe-Mo tetragonal impurity in the parent alloy CoMoFeAl, which is not observed in off-stoichiometric samples.

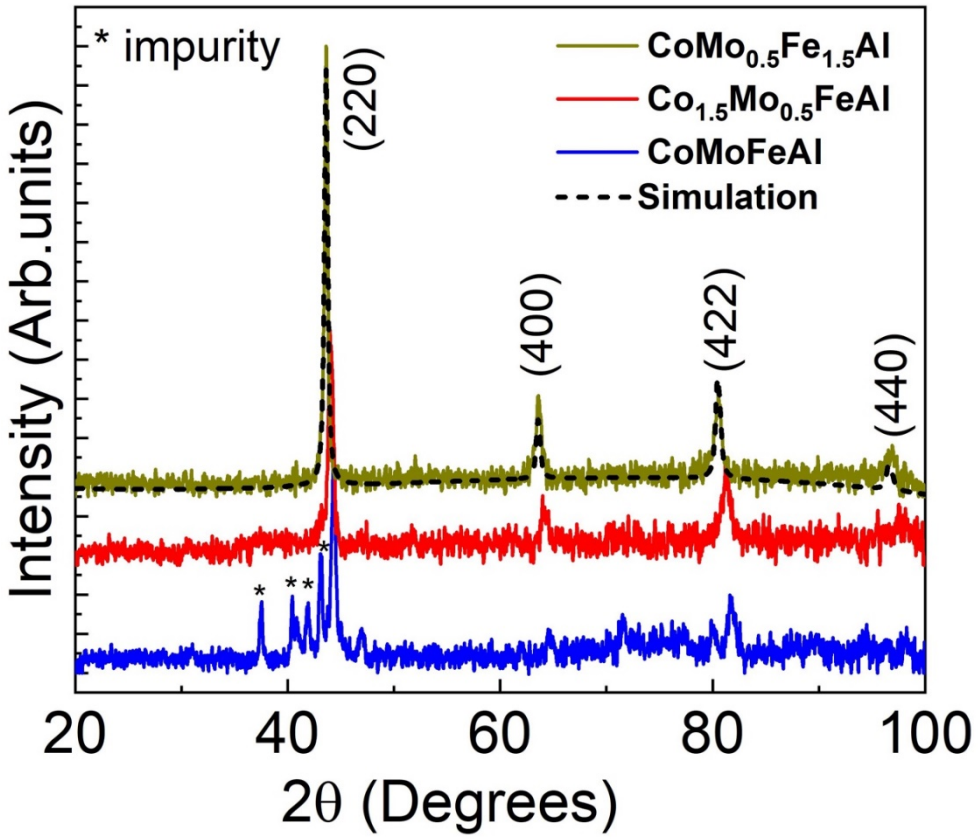


Figure 3: Room temperature x-ray diffraction patterns of CoMoFeAl, $Co_{1.5}Mo_{0.5}FeAl$, and $CoMo_{0.5}Fe_{1.5}Al$ (bottom to top) alloys. The XRD pattern simulated for A2 type disordered structure is shown with dashed line.

Figure 4(a) shows the thermomagnetic curves of the alloys studied. The experiment was done in a constant magnetic field of 1 kOe. All of the alloys have smooth transitions at their Curie temperatures. All compounds have a $T_C$ value much above room temperature with 440 K, 780 K and 950 K for CoMoFeAl, $CoMo_{0.5}Fe_{1.5}Al$ and $Co_{1.5}Mo_{0.5}FeAl$, respectively. The Curie temperatures of the alloys appear to drastically increase when the concentrations of Co and Fe are increased decreasing the amount of Mo. The M(T) curves of all three alloys are similar to those of ferro- or ferrimagnetic materials. Although $Co_{1.5}Mo_{0.5}FeAl$ is predicted to show ferrimagnetic order, we did not see Curie-Weiss behavior to find the type of magnetic ordering as its ordering temperature is close to our highest measurement temperature of 1000 K.

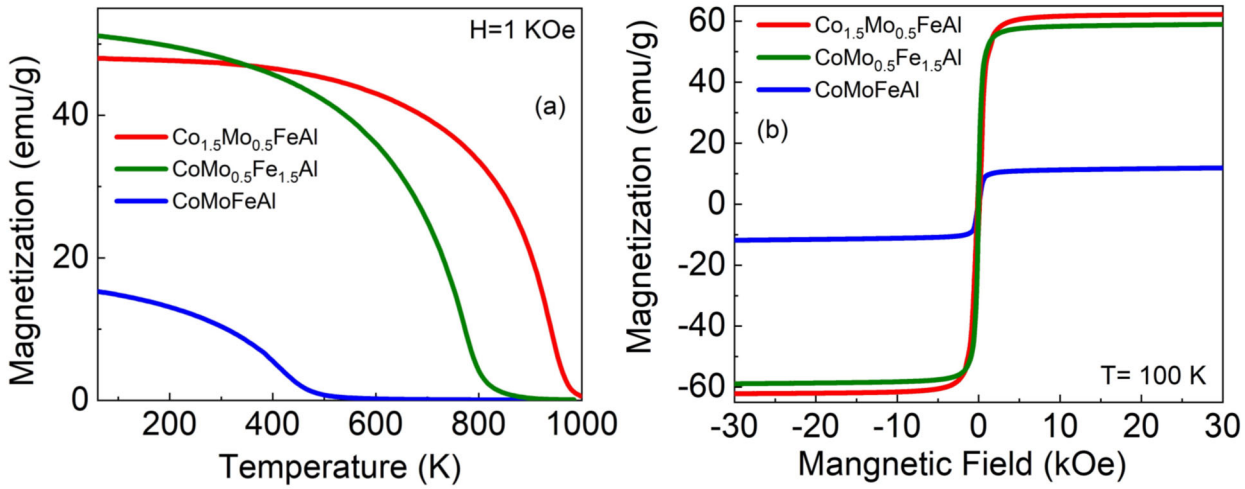


Figure 4: (a) Thermomagnetic curves M(T), and (b) isothermal magnetization curves M(H) of CoMoFeAl, $CoMo_{0.5}Fe_{1.5}Al$, and $Co_{1.5}Mo_{0.5}FeAl$, alloys.

Figure 4(b) shows the isothermal magnetization curves M(H) of the studied alloys measured at 100 K. The saturation magnetizations of CoMoFeAl, $CoMo_{0.5}Fe_{1.5}Al$, and $Co_{1.5}Mo_{0.5}FeAl$ are 12 emu/g ($0.5\,\mu_B/f.u.$), 59 emu/g ($2.3\,\mu_B/f.u.$), and 62 emu/g ($2.4\,\mu_B/f.u.$), respectively. The increase in magnetizations are consistent with the increase in Curie temperature when Mo is partially replaced with Fe or Co. This indicates that the presence of more Fe or Co in the lattice has strengthened the exchange interaction. Although the absolute values of experimental magnetizations are smaller than that of the calculated values, in both cases, CoMoFeAl has the smallest and $Co_{1.5}Mo_{0.5}FeAl$ has the highest values of magnetizations. All studied alloys have very small coercivities. We attribute this discrepancy between theoretical and experimental magnetizations to the observed disorder in the samples.

## IV. Conclusion

We carried out both theoretical and experimental investigations of CoMoFeAl, $CoMo_{0.5}Fe_{1.5}Al$, and $Co_{1.5}Mo_{0.5}FeAl$ Heusler alloys for their structural, magnetic, and electronic band properties. First-principle calculations suggest that CoMoFeAl and $CoMo_{0.5}Fe_{1.5}Al$ are nearly half metallic with spin polarizations of about 80%. The annealed bulk alloys crystallizing in A2 type disordered Heusler structure show high Curie temperatures and moderate saturation magnetization. The saturation magnetizations and Curie temperatures for CoMoFeAl, $CoMo_{0.5}Fe_{1.5}Al$, and $Co_{1.5}Mo_{0.5}FeAl$ are 12 emu/g and 440 K, 59 emu/g and 780 K, and 62 emu/g and 950 K, respectively. Our results indicate that CoMoFeAl and $CoMo_{0.5}Fe_{1.5}Al$ alloys have potential for spintronic applications, and $Co_{1.5}Mo_{0.5}FeAl$ can be used in magnetic applications where soft magnetic properties with high Curie temperature are desired, such as inductive devices.


## Acknowledgments

This research is supported by the National Science Foundation (NSF) under Grant Numbers 2003828 and 2003856 via DMR and EPSCoR. This work used the Extreme Science and Engineering Discovery Environment (XSEDE), which is supported by National Science Foundation grant number ACI-1548562. This work used the XSEDE Regular Memory (Bridges 2) and Storage (Bridges 2 Ocean) at the Pittsburgh Supercomputing Center (PSC) through allocation TGDMR180059, and the resources of the Center for Functional Nanomaterials, which is a U.S. DOE Office of Science Facility, and the Scientific Data and Computing Center, a component of the Computational Science Initiative, at Brookhaven National Laboratory (BNL) under Contract No. DE-SC0012704.


## References


1. T. Graf, C. Felser, S. S. P. Parkin, Simple rules for the understanding of Heusler compounds, Prog. Solid. State Ch., **39**, 1-50(2011).
2. Y. Jin, S. Valloppilly, P. Kharel, R. Pathak, A. Kashyap, R. Skomski and D. J. Sellmyer, Unusual perpendicular anisotropy in $Co_2TiSi$ films, J. Phys. D: Appl. Phys. **52**, 035001(2019).

3. Z. H. Liu, M. Zhang, Y. T. Cui, Y. Q. Zhou, W. H. Wang, and G. H. Wu, Martensitic transformation and shape memory effect in ferromagnetic Heusler alloy $Ni_2FeGa$, Appl. Phys. Lett. **82**, 424 (2003).
4. V. Kumar, N. Kumar, M. Reehuis, J. Gayles, A. S. Sukhanov, A. Hoser, F. Damay, C. Shekhar, P. Adler, and C. Felser, Detection of antiskyrmions by topological Hall effect in Heusler compounds, Phys. Rev. B **101**, 014424 (2020).
5. W. Zhang, P. Kharel, S. Valloppilly and D. J Sellmyer, Large magnetocaloric effect in rapidly quenched $Mn_{50-x}Co_xNi_{40}In_{10}$ nanomaterials, J. Phys. D: Appl. Phys. **54**, 175003(2021).
6. J. Jeong, Y. Ferrante, S. V. Faleev, M. G. Samant, C. Felser, & S. S. Parkin, Termination layer compensated tunnelling magnetoresistance in ferrimagnetic Heusler compounds with high perpendicular magnetic anisotropy, Nat. Commun. *7*(1), 1-8 (2016).
7. K. Elphick, W. Frost, M. Samiepour, T. Kubota, K. Takanashi, H. Sukegawa, S. Mitani, A. Hirohata, Heusler alloys for spintronic devices: review on recent development and future perspective, Science and technology of advanced materials, **22**, 234-271(2021).
8. R. J. Soulen Jr., J. M. Byers, M. S. Osofsky, B. Nadgorny, T. Ambrose, S. F. Cheng, P. R. Broussard, C. T. Tanaka, J. Nowak, J. S. Moodera, A. Barry, and J. M. D. Coey, Measuring the Spin Polarization of a metal with a Superconducting Point Contact, Science **282**, 85 (1998).
9. X. L. Wang, Proposal for a new Class of Materials: Spin Gapless Semiconductors, Phys. Rev. Lett. **100**, 156404 (2008).
10. L. Ritchie, G. Xiao, Y. Ji, T. Y. Chen, C. L. Chien, M. Zhang, J. Chen, Z. Liu, G. Wu, and X. X. Zhang, Magnetic, structural, and transport properties of the Heusler alloys Co2MnSi and NiMnSb, Phys Rev. B **68**, 104430 (2003).
11. M. Jourdan, J. Minár, J. Braun, A. Kronenberg, S. Chadov, B. Balke, A. Gloskovskii, M. Kolbe, H.J. Elmers, G. Schonhense, H. Erbert, C. Felser, & M. Kläui, Direct observation of half-metallicity in the Heusler compound $Co_2MnSi$, Nat. commun. *5*(1), 1-5 (2014).
12. Y. Jin, J. Waybright, P. Kharel, I. Tutic, J. Herran, P. Lukashev, S. Valloppilly, and D. J. Sellmyer, Effect of Fe substitution on the structural, magnetic and electron-transport properties of half-metallic $Co_2TiSi$, AIP Advances **7**, 055812 (2017).
13. P. Kharel, G. Baker, M. Flesche, A. Ramker, Y. Moua, S. Valloppilly, P. M. Shand, and Pavel V. Lukashev, Electronic band structure and magnetism of $CoFeV_{0.5}Mn_{0.5}Si$, AIP Advances **12**, 035011 (2022).
14. I. Tutic, J. Herran, B. Staten, P. Gray, T. Paudel, A. Sokolov, E. Tsymbal, and P. Lukashev, Effects of pressure and strain on spin polarization of IrMnSb, J. Phys.: Condens. Matter **29**, 075801 (2017).
15. A. Nelson, P. Kharel, Y. Huh, R. Fuglsby, J. Guenther, W. Zhang, B. Staten, P. Lukashev, S. Valloppilly, and D. J. Sellmyer, AIP Advances **117**, 153906 (2015).
16. Y. Jin, P. Kharel, S. R. Valloppilly, X.-Z. Li, D. R. Kim, G. J. Zhao, T. Y. Chen, R. Choudhary, A. Kashyap, R. Skomski, and D. J. Sellmyer, Half-metallicity in highly L21-ordered CoFeCrAl thin films, Appl. Phys. Lett. **109**, 142410 (2016).
17. G. Kresse and D. Joubert, From ultrasoft pseudopotentials to the projector augmented-wave method, Phys. Rev. B **59**, 1758 (1999).
18. P. Blöchl, Projector augmented-wave method, Phys. Rev. B **50**, 17953 (1994).
19. J. P. Perdew, K. Burke, and M. Ernzerhof, Generalized Gradient Approximation Made Simple, Phys. Rev. Lett. **77**, 3865 (1996).

20. M. Methfessel and A. T. Paxton, High-precision sampling for Brillouin-zone integration in metals, Phys. Rev. B **40**, 3616 (1989).
21. MedeA-2.22, Materials Design, Inc., San Diego, CA, USA, 2017.
22. J. Towns, T. Cockerill, M. Dahan, I. Foster, K. Gaither, A. Grimshaw, V. Hazlewood, S. Lathrop, D. Lifka, G. D. Peterson, R. Roskies, J. R. Scott, N. Wilkins-Diehr, "XSEDE: Accelerating Scientific Discovery", Computing in Science & Engineering, vol.**16**, no. 5, pp. 62-74, Sept.-Oct. 2014.
23. D. Rani, J. Kangsabanik, K.G. Suresh, and Aftab Alam, Disorder-mediated quenching of magnetization in NbVTiAl: Theory and experiment, J. Magn. Magn. Mater, **551**, 169124 (2022).